ASTRONOMY & ASTROPHYSICS
SUPPLEMENT SERIES

Astron. Astrophys. Suppl. Ser. **108,** 491-508 (1994)

Environments of Seyfert galaxies. I. Construction of the sample and selection effects

E. Laurikainen[1,2], H. Salo[2], P. Teerikorpi[1] and G. Petrov[3]

[1] Turku University Observatory, Tuorla, FIN-21500 Piikkiö, Finland
[2] Department of Astronomy, University of Oulu, FIN-90570 Oulu, Finland
[3] Institute of Astronomy, Bulgarian Academy of Sciences, Sofia, Bulgaria

Received October 28, 1993; accepted June 10, 1994

Abstract. — In order to build a satisfactory picture of Seyferts in relation to normal galaxies we have started a series of papers first establishing some of their basic environmental properties, especially the difference in the number of close companions between Seyfert 1 and Seyfert 2 galaxies. Here we report sample selections and discuss selection effects involved for the samples of 104 Seyferts and 138 control galaxies. The results of the statistical analyses are presented by Laurikainen & Salo (1994, Paper II). The neighbouring galaxies are counted on the Palomar Sky Survey Plates to the limiting magnitude ≈ 19 $m_{\rm pg}$ within the circles of 1.5 Mpc in diameter $\left(H_0 = 100 \text{ km s}^{-1} \text{ Mpc}^{-1}\right)$, large measuring circles enabling good elimination of the background galaxies. Subsamples are selected in order to test the methods by Dahari (1984) and by Fuentes-Williams & Stocke (1988). Elimination of background galaxies and problems related to comparison galaxy sample selection are discussed. The most important problem in our control galaxy sample selection is that the redshifts for most of the control galaxies are unknown. The size of this uncertainty is estimated by determining the redshifts by two ways: (1) by assuming that the selected comparison galaxy has the same redshift as the nearby Seyfert and (2) by Monte-Carlo simulations for Holmberg (1975) galaxy size distribution in space, taking into account the Malmquist bias. The mean redshifts of the comparison sample are estimated with these methods to be 0.028 and 0.029, respectively, compared with 0.026 for the Seyfert sample. Distribution of Seyferts in Zwicky's clusters is also addressed, and compared with previous studies. Taking into account optical projections, about 3/4 of the Seyferts are found to be field galaxies. Galaxies in clusters lie preferentially at the cluster borders.

Key words: galaxies: clustering; interactions; Seyfert — methods: statistical

1. Introduction

One of the proposed mechanisms to explain the large energies in active galactic nuclei (AGN) is based on the hypothesis that many galaxies have massive black holes in their nuclei. These nuclei turn active only when refueled by an interaction which delivers gas to be captured near the galactic center and finally falling into the black hole (Osterbrock 1993). In an alternative picture AGN are photoionized by very hot stars rather than by a central massive object (Terlevich & Melnick 1985). In both cases we might expect to find an excess of AGN in galaxies having nearby companions, or among interacting or disturbed systems.

There is a strong evidence that many Seyfert galaxies are distorted (Vorontsov-Velyaminov 1977; Adams 1977; Wehinger & Wyckoff 1978), and that many of them have bars (Heckman 1978; Simkin et al. 1980). However, they seem to avoid extremely distorted systems (Dahari 1985; Keel et al. 1985; Bushouse 1986). Several statistical studies have found an excess of Seyferts with nearby neighbours compared with nonactive galaxies (Petrosian 1982; Dahari 1985, MacKenty 1989). This seems to suggest some correlation between tidal interactions in triggering the nuclear activity, but it is not clear whether this is the dominant mechanism. Indeed, the contrary result showing only a marginal excess of neighbours among Seyferts has also been obtained (Fuentes-Williams & Stocke 1988).

The present paper starts a series of studies where we first try to understand the controversial results concerning the Seyfert galaxy environments and then to correlate the morphological features and environmental properties with the dynamical states of the galaxies. The final goal is to build a satisfactory picture of Seyferts in relation to normal and other types of active galaxies. In this paper we present our sample selection, discuss possible selection effects and study galaxy memberships in Zwicky's clusters. Paper II (Laurikainen & Salo 1994) in the series is devoted

to a detailed analysis of the galaxy environments. In Paper II we found that Seyferts 2 galaxies have more companions than the control galaxies, but that Seyferts as a whole do not appear more frequently in interacting systems. We use the Hubble constant $H_0 = 100$ km s^{-1} Mpc^{-1} throughout the paper if not otherwise mentioned.

2. Sample selection

The principal Seyfert- and comparison galaxy samples (Sy, comp in the Tables) were compiled and their environments studied from the blue Palomar Sky Survey plates (POSS). Our main idea is to have a sufficiently large circles around the Seyferts, allowing accurate estimation of background galaxy densities, and a direct comparison of different Seyfert types. In order to compare our results with those obtained by Dahari (1984) and Fuentes-Williams & Stocke (1988, hereafter FWS) and to check how much projections on galaxy clusters affect the results, suitable subsamples were compiled.

2.1. *Seyferts*

The Seyfert sample was compiled from the list of Dahari & de Robertis (1988), which includes galaxies north of $\delta = -30°$ at $z < 0.05$. Their sample of 152 Seyferts includes 83% of all known Markarian Seyferts and a majority of the classical Seyferts listed by Weedman (1977, 1978). Their Seyfert classifications are from the discovery papers which may not necessarily agree with Osterbrock's criteria (see Shuder & Osterbrock 1981; Osterbrock 1984). The spectroscopic database by Dahari & de Robertis, largely based on their own observations, is the most uniform available in the literature. This is important for our further use of the sample. Additionally we applied the following selection criteria: (1) $0.01 < z < 0.043$ and (2) galaxies that did not fulfill Osterbrock's criteria for Seyferts were eliminated. The nearest galaxies were excluded to facilitate measurements on the POSS plates, and very distant objects were eliminated, as statistics would be too poor and the morphological types difficult to determine. Osterbrock's criteria were used in order to build a homogeneous sample of Seyferts without marginal LINERs or starburst galaxies. Our final sample consists of 104 Seyferts, of which 55 are Seyfert 2 and 49 Seyfert 1 galaxies including also intermediate types. In the following the types 1−1.5 will be considered as Seyfert 1, and the types 1.8−2.0 as Seyfert 2 galaxies. The samples and some physical parameters of the galaxies are shown in Table 1. The columns are the following:

1) Galaxy name,
2) Redshift,
3) Morphological type,
4) Seyfert type,
5) Visual apparent magnitude,
6) Measured diameter in millimeters, with the accuracy of 0.025 mm,
7) Major and minor axis diameters in blue color taken from the literature or estimated from our own measurements,
8) Minor to major axis ratio calculated using the catalogued diameters when available. For the rest of the galaxies we used the ratios measured by Dahari & de Robertis from the red POSS plates.

Morphological types of Seyferts are from the Catalog of Markarian Galaxies (Mazzarella & Balzano 1986) when available and otherwise from the Second Reference Catalogue of Bright Galaxies (de Vaucouleurs et al. 1976) and from NASA/IPAC Extragalactic Database (NED). Redshifts are taken from the Catalogue of Principal Galaxies (Paturel et al. 1989) and from NED for the low-redshift comparison galaxies, and from Dahari & de Robertis (1988) for the Seyferts. The visual apparent magnitudes were taken from NED for all galaxies. Figure 1 displays the diameter, redshift and absolute magnitude distributions of the final Seyfert sample, showing the two Seyfert types and the morphological types separately. Note that there is a rather significant redshift difference between the early-type Seyfert 1 and Seyfert 2 galaxies, which is however largely reduced while limiting to galaxies at $z \leq 0.03$. The mean properties of the selected sample of Seyferts and of all the other samples (see Sect. 2.3) are shown in Table 2.

2.2. *Comparison galaxies*

In principle, the control sample should include galaxies with the same distribution of Hubble types, redshifts and absolute magnitudes as the Seyferts so that environments of identical parent galaxies could be compared. This kind of attempt was made by FWS, but unfortunately they had a large bias between the redshift distributions of Seyferts and comparison galaxies. Also, if the nuclear brightnesses of the galaxies are not known this kind of sample selection is somewhat risky. Namely Granato et al. (1993) and Kotilainen & Ward (1993) have shown that nuclear brightnesses of Seyfert 1 galaxies may account even 90% of the total galaxy luminosity. Accordingly, matching the compared samples in total absolute magnitude would bias the comparison sample towards larger and brighter galaxies. Even matching the parent galaxy magnitudes would be dangerous: if galaxy interactions play an important role in triggering Seyfert activity the parent galaxy may temporarily brighten due to increased star formation in the galactic disk as shown by Schombert et al. (1990) and Laurikainen et al. (1993). For the majority of the galaxies in our Seyfert sample the nuclear luminosities are not known.

An alternative would be to construct a comparison sample matching Seyferts in diameter, redshift and

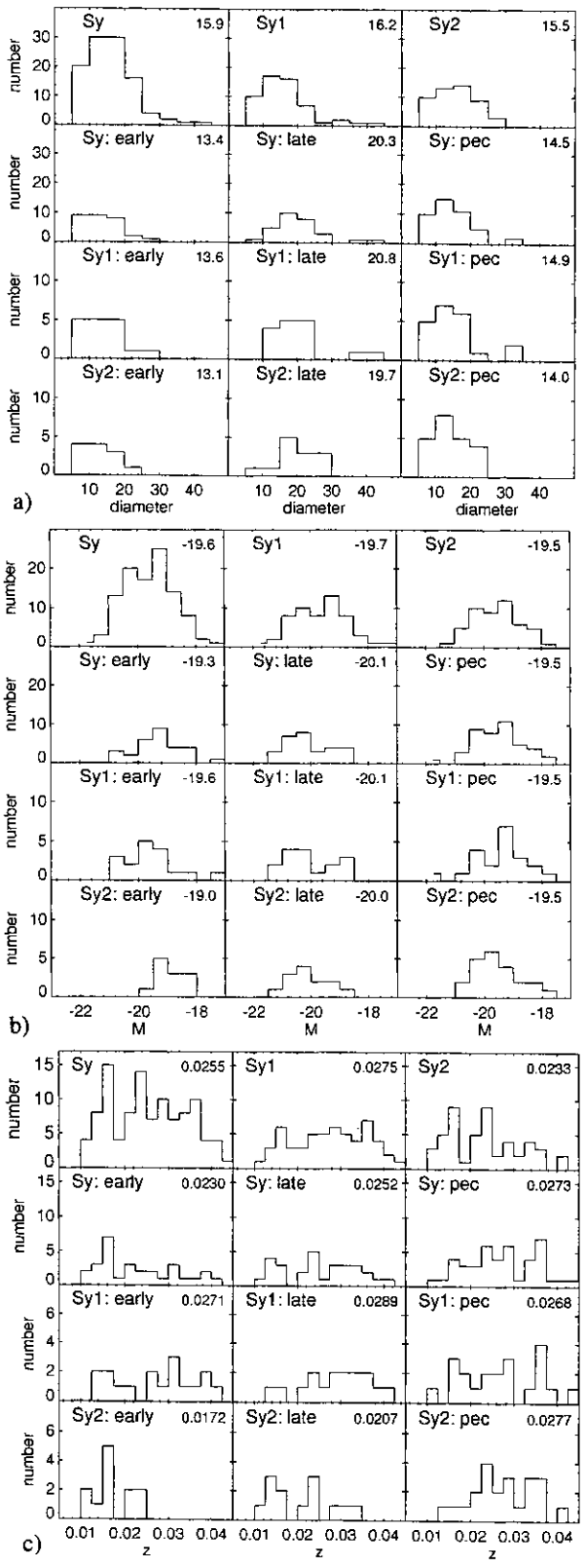

Fig. 1. Distribution of a) diameters in kpc, b) absolute visual magnitudes and c) redshifts for various subsets of our Seyfert sample. Mean values are indicated in the frames. Early-type galaxies include E+SO galaxies, late-types Sa–ScI spirals and pec galaxies are classified as peculiar

morphological type, as the diameters are not influenced by the nuclear brightness. Data in the redshift catalogue by Huchra et al. (1983) would enable this kind of sample selection. However, we preferred Dahari's (1984) method of sample selection in order to understand his result. Accordingly, the control sample was assembled using only an apparent dimension criterion: for each Seyfert two closest neighbours were chosen, one spiral and one early-type galaxy (E+SO) having major axis diameter D_c in the range: $0.65D_{Sy} < D_c < 2.00D_{Sy}$, where D_{Sy} is the apparent major axis diameter of the Seyfert galaxy (note that Dahari used the selection criterion $0.75D_{Sy} < D_c < 1.5D_{Sy}$). Unfortunately most of the redshifts of the comparison galaxies are unknown.

The comparison galaxies were searched from the same POSS plates as the Seyferts, but if no objects within the allowed diameter range appeared, adjacent plates were investigated. As this happened in a very few cases only the possible seeing differences between the POSS plates are not expected to have significant effect on the statistics. In a very few cases no early-type galaxy was found and it was replaced by a spiral. As most of the Markarian galaxies are Seyferts or harbour a starburst in their nuclei only non-Markarian galaxies were accepted. For the selected comparison galaxies the environments were measured for 75 spirals and 63 early-type galaxies which comprise the final comparison sample.

Dahari excluded galaxies in or near the centers of rich clusters because the central galaxies may have very uncommon physical properties. Our comparison sample is also free of this kind of galaxies. Dahari also limited his samples to more nearby objects ($z < 0.03$) than we did ($0.01 < z < 0.043$). In our study the most nearby galaxies were excluded, because it would have been unreasonable to count absolutely very small neighbouring galaxies only for a few galaxies. Another difference in our sample selection is that we took one early-type and one late-type galaxy in the vicinity of every Seyfert, whereas Dahari selected the control galaxies randomly. It is not clear for us why Dahari found practically no physical companions around his control galaxies: he detected the same number of neighbouring galaxies around the comparison galaxies as expected according to the probability function for optical superpositions. We believe that our comparison sample is more reasonable, as the projected surface density of neighbouring galaxies (Fig. 2) is consistent with the standard galaxy auto-correlation models (e.g. Lake & Tremaine 1980).

The advantage of our comparison sample is that we can test directly the Dahari's method. The weakest point is that the redshifts for a large majority of the comparison galaxies are not known, implying that the absolute magnitudes of the galaxies and the true linear sizes of the counting circles are also uncertain. This problem will be discussed in detail in Sect. 5.2.

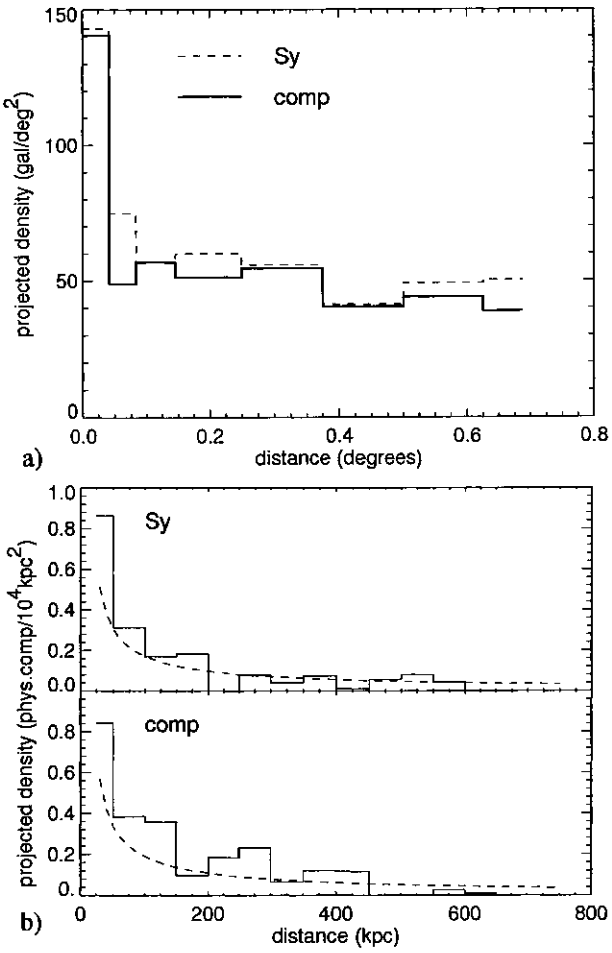

Fig. 2. a) Projected surface densities of measured neighbours (number/main galaxy/deg^2) as a function of angular separation from the central galaxy, shown for Seyferts with $z < 0.02$, and for comparison galaxies with known redshifts. Limiting size for the neighbours is 0.2 mm (see Fig. 3). Our measurement circle with radius 750 kpc corresponds to ≈ 0.7 degrees at $z = 0.02$. b) Projected surface densities of physical companions (number/main galaxy/(100 kpc)^2) as a function of distance from the central galaxy, together with the projected density calculated from the Lake-Tremaine auto-correlation model (dashed curves, assuming $\rho(d) \propto (d/3.8\ \mathrm{Mpc})^{-1.8}$). The background calculated in the zone 500–700 kpc has been subtracted, and the curves are fitted to the density at the zone 300–500 kpc

2.3. *Other samples*

Additionally we selected the following subsamples (see Table 2):

1) Seyfert 1 and Seyfert 2 galaxies (Sy1, Sy2),

2) samples imitating Dahari's selection criteria,

3) samples imitating FWS z-distributions ($Sy_{\mathrm{high}\ z}$, $Sy_{\mathrm{low}\ z}$),

4) samples to check effects of projection on Zwicky's clusters (Sy_{proj}, $Sy_{\mathrm{non\text{-}proj}}$).

The principal Seyfert sample consisting of all Seyfert galaxies used in this study was divided to type 1 and type 2 objects, their mean redshifts and morphological distributions being rather similar.

The sample selection criteria by Dahari and by us are so similar that in order to compare the results we need only to restrict our minimum companion galaxy size to that in Dahari's measurements. Unfortunately he did not give it so that we tried to estimate the minimum measured size indirectly. According to Dahari, 37% of his Seyferts have at least one neighbour within $3D_{\mathrm{Sy}}$ (31 out of 84). From our data for Seyferts at $z < 0.03$, 46% have companions if the size ≥ 0.2 mm, and 31% if the size ≥ 0.3 mm, suggesting that Dahari's measurements extend to the minimum size of ≈ 0.25 mm. This is in agreement with the estimates of background densities compared to Lick counts.

To imitate FWS's sample selection we should be able to do it according to known redshifts, absolute magnitudes and morphological types, which is not possible. Anyway we believe that the biggest problem in the analyses by FWS is that their Seyfert- and comparison galaxy samples are not comparable in redshift, the mean redshifts being 0.0307 and 0.0193, respectively. This implies that they measure on the average 2.5 times larger environments for their control galaxies than for the Seyferts. On the other hand, they count a larger fraction of background galaxies around Seyferts as physical companions, due to the reasons explained in Sect. 5.1. To look at what is the net effect of these competing tendencies our Seyfert sample was divided into low- and high redshift subsamples the mean redshifts being consistent with those of FWS's Seyfert and comparison samples.

3. Measurements

The angular diameters of the galaxies were measured from the blue POSS plates, using a 25-power magnifier with a scale divided to 0.025 mm corresponding to 1.7 arcsec (on the POSS plates 1 mm corresponds to 67.14 arcsec). The boundary of each galaxy was defined as the faintest envelope visible on the plate, in accordance with Dahari (1984).

The numbers of galaxies around the Seyferts and the comparison galaxies were counted in circles with a diameter of 1.50 Mpc (for $z = 0.01$ this corresponds to 154 mm circle at POSS plates). The neighbouring galaxies were roughly identified as spirals or early-type galaxies, and their angular diameters and distances from the central galaxies were measured. Accuracy of the distance measurements was the same as for the angular diameters near to the main galaxy (about 0.05 mm), whereas for distant objects (more distant than $20 - 30D_{\mathrm{gal}}$) it was one millimeter, sufficient for the present purpose. Morphological classification of the neighbouring galaxies turned out to be very inaccurate, evidenced by the fact that the fraction of

spirals correlates with the measured size. Therefore morphological classifications of the neighbouring galaxies will not be used in the following. The measurements turned out to be complete to the limiting size of 0.2 mm as shown in Fig. 3 (0.2 mm at $z = 0.01$ corresponds to $M_{pg} = -13.5$ and at $z = 0.04$ to $M_{pg} = -16.5$). The measurements are homogeneous throughout the counted area, evidenced by the fact that the mean measured galaxy size is independent of the distance from the central object, except within a distance of a few main galaxy diameters, where we expect to see mainly physical companions.

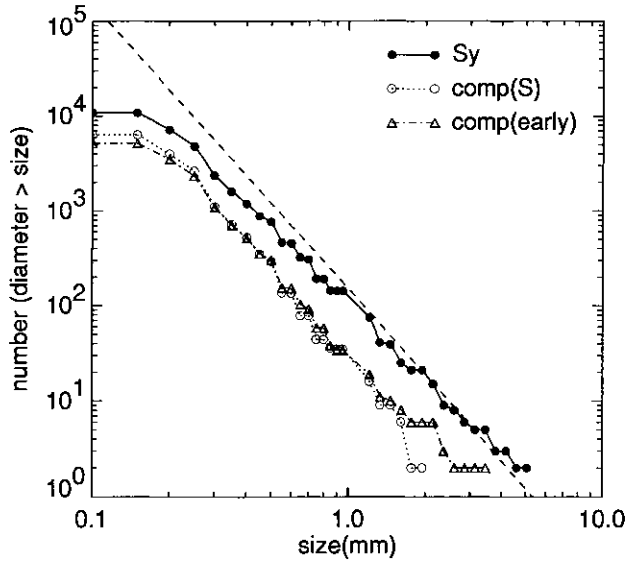

Fig. 3. Cumulative distribution of measured companion diameters, shown separately for neighbourhoods of three different main galaxy samples: Seyfert sample, spiral comparison sample (Sa–ScI), and early type comparison sample (E+SO), denoted by Sy, comp (S), and comp (early), respectively. The same designations are used in the subsequent figures. The dashed line with logarithmic slope −3 indicates the expected relation for a complete sample, showing that for size < 0.20 mm our measurements are severely incomplete: these small companions are excluded from our analysis

For comparison with FWS's results we also need to estimate the Holmberg diameters. The measured galaxy diameters were converted to a homogeneous system, chosen to be that used in the Uppsala General Catalogue of Galaxies (Nilson 1973). For Seyferts, as well as for both types of comparison galaxies the following relation was found (see Fig. 4):

$$D_{corr} = 1.2 \times D_{meas} + 0.1 \text{ mm}$$

As the correction term is near to the Holmberg correction 1.46 for intermediately elongated galaxies (Holmberg 1975) it will be called as Holmberg correction hereafter. The correction term for our galaxies was found to be independent of the galaxy inclination. In the following we use

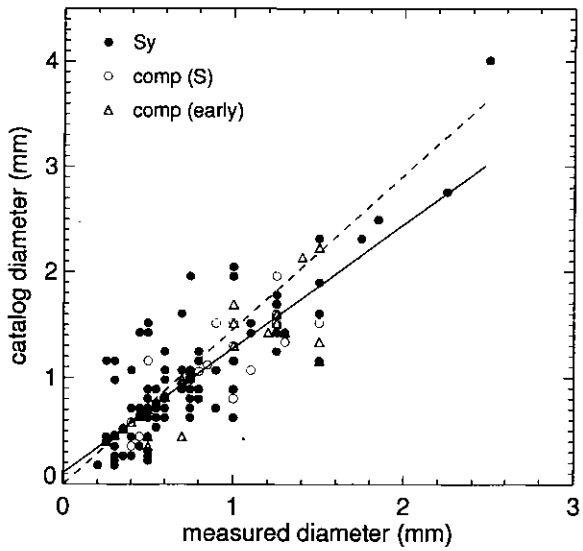

Fig. 4. Relation between measured major axis diameter and that derived from the Uppsala General Catalog of Galaxies (Nilson 1973). Solid line denotes the least-square fit to all data points, $y = 1.2 * x + 0.1$ mm, while dashed lines show the Holmberg-relation, $y = 1.46 * x$

uncorrected diameters, if not mentioned to be Holmberg diameters.

4. Background galaxies

The lack of proper elimination of background galaxies is a serious weakness in most of the statistical studies performed of the environments of Seyfert galaxies. Even if the background is taken into account (Dahari 1984) its resolution is usually less than for the counts in the immediate galaxy neighbourhoods. In our database it is the same for both purposes so that we can test how much poor resolution of the background galaxy density affects the results. The contamination by background galaxies was estimated by two different ways:

1) by the Lick counts of galaxies (Shane 1975) and
2) estimates from the POSS-plates at a projected distance of 500–700 kpc from the central galaxy.

The estimates of the background galaxy numbers by Lick counts were made in order to verify Dahari's result. Shane (1975) published maps of the projected local densities of galaxies, based on the Lick counts, extending down to $m_{pg} = 18.8$. In order to use the Shane maps we must determine the correlation between his counts and our POSS plate measurements. The comparison was made by integrating over the surface area corresponding the measured region on the POSS plate. The POSS counts were found to yield mean galaxy surface densities almost similar to those in Shane's maps (POSS/Lick = 1.1), when neighbouring galaxies above the completeness limit 0.2 mm were considered. Using the relation:

$$d\left(\log_{10}N(m)\right)/dm = 0.6,$$

where $N(m)$ is the number of galaxies of magnitude m or brighter per unit solid angle, we find the measurements to be complete down to the limiting magnitude 18.9 m_{pg}. In the original database the magnitude limit is 19.1, being 0.8 magnitudes fainter than in Dahari (1984).

The background galaxy densities obtained from Shane's maps and from our measurements have very weak or no correlation at all ($r = 0.17$) as shown in Fig. 5. The dispersion is equally large for galaxies projected on Zwicky's clusters as for non-cluster galaxies. However, it is evident that the background densities obtained from the POSS plates are more accurate than those derived from Shane's maps. This is illustrated in Fig. 6, where the estimated number of physical neighbours of Seyfert galaxies, N_{comp}, is plotted as a function of redshift after applying the two ways of eliminating the background galaxies (left and middle panels). The Lick counts were corrected to the limiting magnitude of the POSS measurements. The higher dispersion when the background is derived from the Lick counts is probably due to the low resolution of the maps: in the Lick counts the galaxy numbers are given for areas of one square degree, while our counts refer typically to areas of 0.2 square degrees. Figure 6 (right panel) illustrates that the dispersion in N_{comp} diminishes even more dramatically when galaxy sizes smaller than 5.7 kpc are excluded. This limit corresponds the minimum galaxy size detectable at the redshift 0.03 (corresponding to the angular size 0.2 mm) thus enabling more homogeneous inspection of companions throughout the whole redshift range considered.

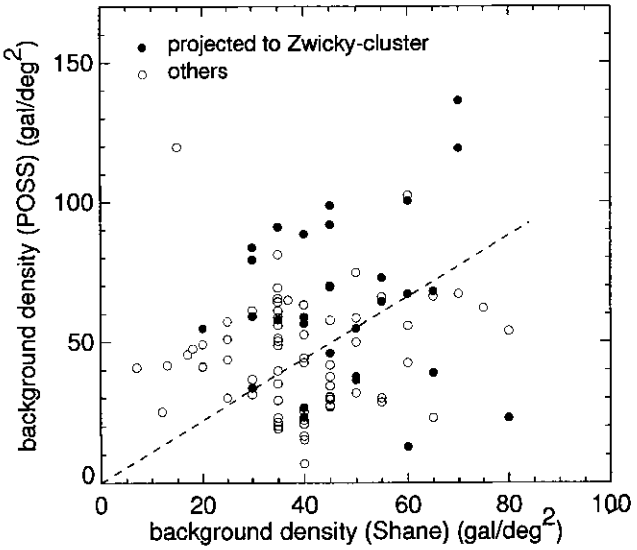

Fig. 5. Relation between the projected galaxy density in Lick counts and in our measurements from POSS-plates. Dashed line shows the approximative relation $\rho_{POSS} = 1.1 \times \rho_{Lick}$

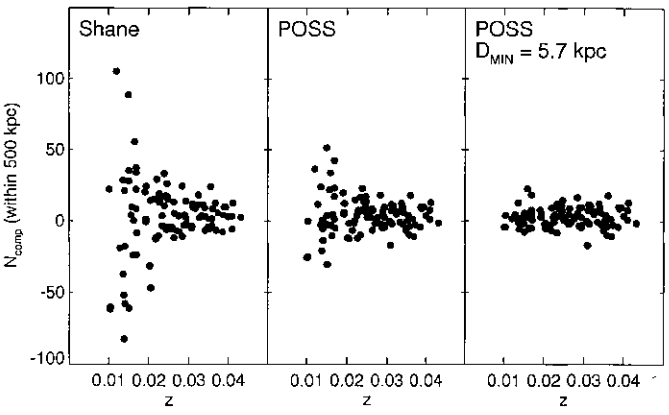

Fig. 6. Estimated number of physical neighbours within the projected distance of 500 kpc from the Seyfert galaxy as a function of redshift. In the middle panel the background was estimated from the measured number of neighbours in the POSS plates in the zone 500−700 kpc. In the left hand panel the Lick counts were used, with the correction $\rho_{POSS} = 1.1 \times \rho_{Lick}$. On the right only galaxies with diameter $\geq$ 5.7 kpc are included and the appropriate background is taken from POSS

5. Selection effects

5.1. *The problem of the background galaxies*

The background galaxy problem is roughly the following: as the background galaxy surface density is independent of the distance, the number of galaxies within a certain assigned absolute diameter range generally increases with redshift. Therefore any bias in redshift between the compared samples easily introduces errors.

Let us assume that the background galaxy density of galaxies larger than θ (apparent size) is given by

$$\rho(>\theta) \propto \theta^{\alpha}, \tag{1}$$

where $\alpha = -3$ in the classical case of a homogeneous space distribution. The corresponding differential distribution is

$$d\rho/d\theta \propto c\theta^{\alpha-1}. \tag{2}$$

One often restricts the "true" companions to lie within a fixed linear size range $D_{min} \leq D \leq D_{max}$, where the distance is assumed to be that of the central galaxy (e.g. FWS). Then for a galaxy at redshift z the number of these "companions" provided by the mere background galaxies, is proportional to

$$N_{opt}(z) \propto \int_{kD_{min}/z}^{kD_{max}/z} \theta^{-4}\mathrm{d}\theta \propto z^3\left(D_{min}^{-3} - D_{max}^{-3}\right), \tag{3}$$

where $k = H_0/c$. Then the number of galaxies counted in a circle with a fixed linear size, say R_c, will be

$$N_{gal}(z,\ R_c) \propto z^{-2}z^3 \propto z. \tag{4}$$

Clearly, the number of false companions increases with the redshift as smaller and smaller galaxies are included. This is illustrated in Fig. 7 showing the Holmberg corrected angular diameters of the neighbouring galaxies of Seyferts's as a function of redshift. The minimum and maximum galaxy sizes of the so called "associated" galaxies, considered as physical companions in FWS are shown in the diagram (15 and 50 kpc). Figure 8 plotting $N_{\rm neigh}$, the number of associated galaxies as a function of redshift, shows the same thing more quantitatively (it is interesting to note that this growth in galaxy number approximately follows that found by FWS while comparing their low-redshift comparison sample ($z = 0.0192$), the higher redshift Seyfert sample ($z = 0.0307$) and the radiogalaxy sample ($z = 0.0602$), implying that background galaxies may dominate their results). Note that $N_{\rm comp}$ which was used in Sect. 4.2 is different from $N_{\rm neigh}$, the former estimating the number of physical companions with proper background elimination.

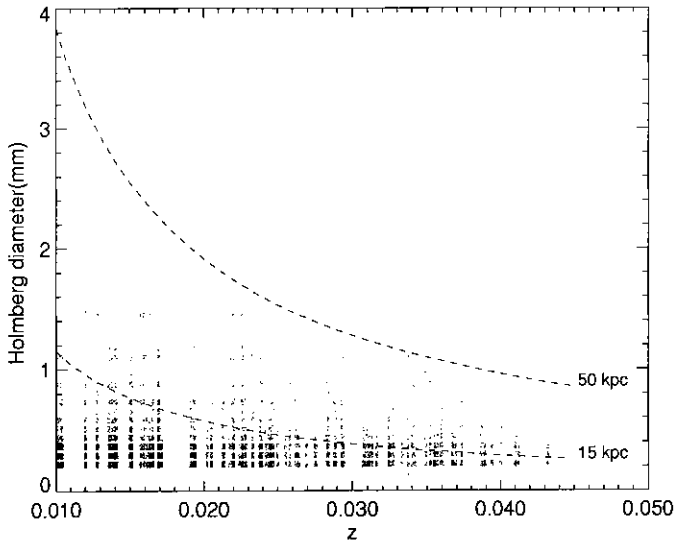

Fig. 7. The FWS method for estimating the number of physical companions is analyzed. The measured diameters (with Holmberg correction) of Seyfert neighbours are shown as a function of Seyfert redshift. The dashed lines indicate corresponding physical sizes for $H_0 = 75$ km s^{-1} Mpc^{-1}. In order to make individual measurements visible, small random shifts have been added to each data point

The above formula is valid as long as $kD_{\rm min}/z > \theta_{\rm lim}$, or $z < z_{\rm max} = kD_{\rm min}/\theta_{\rm lim}$, where $\theta_{\rm lim}$ is the minimum angular size measured. For $z > z_{\rm max}$,

$$N_{\rm opt}(z) \propto \theta_{\rm lim}^{-3} - z^3\,(kD_{\rm max})^{-3}\,, \qquad (5)$$

and the contribution from the background starts to diminish. With $\theta_{\rm lim} = 0.2$ mm $\times\ 67''/{\rm mm} = 13.4''$ and $D_{\rm min} = 15$ kpc ($H_0 = 75$ km s^{-1} Mpc^{-1}, as used by FWS), the

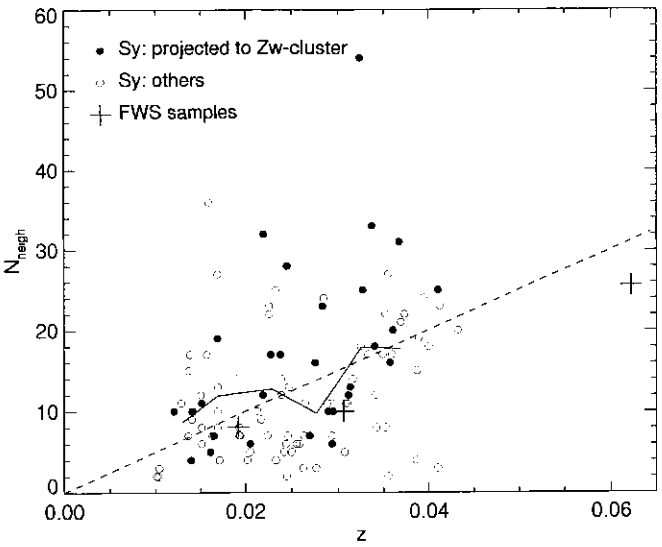

Fig. 8. Following FWS, all galaxies with 15 kpc $\leq D_{\rm Holm} \leq$ 50 kpc are assumed to be physical companions: their number is presented by open and filled circles for the Seyferts, together with the mean value over different z-bins (solid line). Also shown is the least-square linear fit to the data, constrained to go through the origo (dashed line). (As discussed in the text, the method is expected to yield unphysical relation, $N_{\rm neigh} \propto z$, in accordance with the plot). Also shown are data from FWS for their three different data sets (large crosses) following the same trend

redshift limit becomes $z_{\rm max} = 0.058$ which is larger than our upper limit $z = 0.043$. With $H_0 = 100$ km s^{-1} Mpc^{-1} and $z_{\rm max} = 0.043$, corresponding to our upper redshift limit, the lower limit for where Eq. (4) still applies becomes $D_{\rm min} = 8.3$ kpc.

In addition to the false companions one expects true companions in the counting circle. Assume a common size distribution function $\Psi(D) = c_1 D^\beta$ for the true companions, with the constant c_1 equal for different host galaxies. If we are again interested in companions within certain size limits, then at the redshift z the number of companions becomes

$$\begin{aligned} N_{\rm c}(z) &= c_1 \int_{D_{\rm min}}^{D_{\rm max}} D^\beta {\rm d}D = \text{constant}, \quad z < z_{\rm max}\,(D_{\rm min})\,, \\ &= c_1 \int_{z\theta_{{\rm min}/k}}^{D_{\rm max}} D^\beta {\rm d}D = c_1/(\beta+1) \qquad (6) \\ &\left(D_{\rm max}^{\beta+1} - (\theta_{\rm lim} z/k)^{\beta+1}\right), \qquad z > z_{\rm max}\,(D_{\rm min}) \end{aligned}$$

Hence the counted number of true companions is either constant or decreases with increasing z (assuming $\beta + 1 < 0$), depending on the adopted $D_{\rm min}$. Without any imposed limits other than the lower angular size limit $N_{\rm gal} \propto z^{-2}$ and $N_{\rm c} \propto z^{\beta+1}$. Now if $(\beta+1) < -2$ or $\beta < -3$, the fraction

of true companions will decrease with increasing z. This condition should be valid in the bright end of the general diameter function as derived by Karachentsev et al. (1972) where the slope ≈ -4. However, around $D = 10$ kpc there is a change towards significantly more shallow slope, and it is possible that at sufficiently small z the fraction of true companions first increases.

In order to put these estimates into more quantitative grounds we need to adopt some specific distribution function for the companion galaxy diameters. Figure 9 displays the magnitude distribution derived by Holmberg (1975), and the corresponding diameter distribution where the relation $M = -6 \log A + 7.14$ has been used (A is the galaxy diameter in parsecs). For comparison, the measurements by Karachentsev et al. (1972) are also displayed, together with lines corresponding to slopes -4 and -1. Holmberg's curve was originally based on the examination of groups around nearby spirals, but it also matches with the general size distribution of galaxies with known redshifts (Holmberg's redshift lists were complete down to $m_B \approx 12$. We also checked this with the more extensive redshift data now available in the redshift catalogue by Huchra et al. (1983), complete down to $m_B \approx 13$). Note that this distribution is different from the Schechter-law, which describes the distribution of *bright* galaxies.

With the help of Holmberg diameter function we can evaluate the integral (6) for various $\theta_{\rm lim}$, and estimate the z-dependence of $N_{\rm c}/N_{\rm gal}$ in a fixed measurement circle.

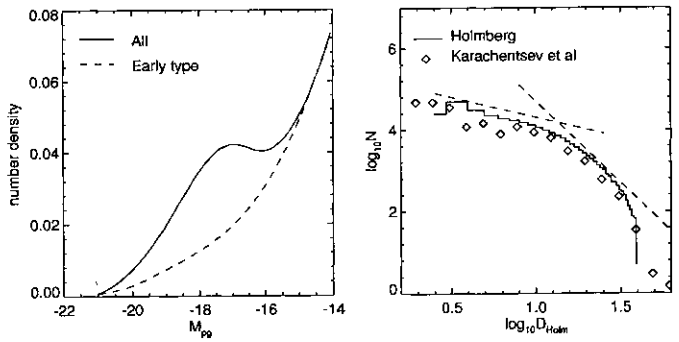

Fig. 9. In a) the Holmberg (1975) absolute magnitude distribution function is shown, based on measurements of neighbourhoods of nearby spirals. Solid line shows all the galaxies whereas dashed line refers to early-type galaxies. In b) the magnitude distribution is converted to diameter distribution, with Holmberg relation $M = -6 \log_{10}\left(D_{\rm kpc}\right) - 10.86$. Also shown are measurements by Karachentsev et al. (1972), together with dashed lines indicating slopes -4 and -1 (following Holmberg $H_0 = 80$ km s^{-1} Mpc^{-1} is assumed in this figure). In both frames vertical scales are arbitrary

This is shown in Fig. 10, and compared with the data obtained from the measurements around Seyfert 2 galaxies. The fractions are normalized to 100 kpc circles with the measurements for $\theta_{\rm lim} = 0.2$ mm, and $0.01 < z < 0.02$. For $\theta_{\rm lim} = 0.2$ mm, the fraction of physical companions is expected to increase monotonically for our z-interval, whereas with larger $\theta_{\rm lim}$ (corresponding to larger absolute diameters of true companions) it first increases but then turns to decrease at larger z. Actual measurements, although showing large dispersion, agree with these trends. For our purpose the most important feature of the curves is the fairly uniform fraction of expected true companions, varying only by a factor of 2–3 for z between 0.01 and 0.04. The shapes of the curves are rather sensitive to the assumed size distribution: for example if smaller companions were made more abundant, the turn in the slope would occur at smaller z's, making the overall variations much larger. This can be ruled out as the agreement with measurements would then be much poorer. Also shown is the curve where the physical sizes are further restricted to be > 5.7 kpc, in which case $N_{\rm c}/N_{\rm gal}$ is largest for small z (in this case $N_{\rm c}$ is constant for $z < z_{\rm max}$, whereas due to the diameter limit, $N_{\rm gal} \propto z$, see Eq. (4)).

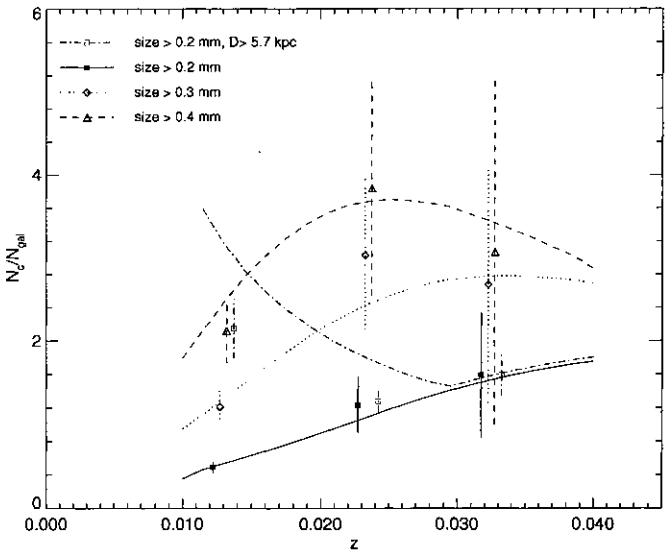

Fig. 10. Relative fraction of physical companions as a function of redshift for 100 kpc measurement circles. Curves indicate estimates for various limiting apparent sizes, and are based on Holmberg's size distribution function for companion galaxies. Symbols stand for measurements around Seyfert 2 galaxies in three redshift bins. Error bars (with length of 0.5 standard deviations) indicate variance among galaxies in each bin. Normalization is made according to the measurements with size limit 0.2 mm for $0.01 < z < 0.02$

In conclusion, the detection of optical companions is strongly redshift dependent, whereas the detection of physically associated galaxies depends on the galaxy luminosity function and therefore also on the absolute magnitude range considered. However, our estimates imply that the fraction of true companions should behave in a tolerably uniform fashion throughout the z-interval covered by the samples, thus making the accuracy of the background galaxy elimination reasonable.

5.2. *Redshift distributions*

The problem of matching the redshifts exists between our principal comparison and Seyfert samples whereas for the Seyfert subsamples redshift is one of the selection criteria. As the comparison galaxies were selected on the basis of their angular sizes following those of Seyferts we must consider how well this constraints their redshift distributions: any systematic difference in the absolute mean linear sizes will induce a similar redshift difference. Two major problems arise, related to two types of Malmquist bias.

First, it is expected that there is a systematic increase in size of the Seyferts when z is increased (distance-dependent Malmquist bias). The selection arises as only brighter and therefore presumably larger Seyferts are detected at larger redshifts. Secondly, $\langle D\rangle_{\rm gal}$, the average linear size of the comparison galaxies chosen by fixed angular diameters, is actually larger than the average linear size $\langle D\rangle_0$ of a volume limited sample of normal galaxies (the classical Malmquist-effect). This follows from the fact that a galaxy with a given angular size can be a nearby small galaxy or a more distant large one. As the volume occupied by the distant galaxies is larger, they dominate and increase the mean linear diameter. The effect is independent of the angular size and therefore the bias is the same for the comparison galaxies of low- and high redshift Seyferts. This simplifies the analyses, but two relevant questions remain:
1) How large is this constant bias? and 2) is there any distance dependent bias in the Seyfert sample?

The distance dependent Malmquist effect for diameters is rather insignificant in our Seyfert sample (Fig. 11): $\langle D\rangle_{\rm Sy}$ for $z < 0.02$ is 15.4 kpc while for the whole sample $\langle D\rangle_{\rm Sy} = 15.9$ kpc. Also, the least squares fit indicates only about 10% increase in size between $z = 0.01 - 0.04$. However, the corresponding bias in absolute magnitudes is much larger and is addressed in next section.

In principle, for a narrow, centrally peaked size distribution the amount of Malmquist effect can be estimated analytically, the ratio of the average diameters becoming

$$\langle D\rangle_{\rm gal}/\langle D\rangle_0 = 1 + 3.5\ \sigma^2_{\log D}, \qquad (7)$$

where $\sigma_{\log D}$ is the gaussian dispersion of log D for the galaxies in question (Lynden-Bell et al. 1988). However, in reality this result depends on the form of the size distribution function of galaxies. We can again use Holmberg (1975) distribution, based on galaxy measurements to estimate this correction for our comparison galaxies. Figure 12 illustrates the results from a Monte-Carlo simulation where a spherical volume extending to z =0.15 was filled uniformly with N=100 000 galaxies following the Holmberg size distribution (simulation was performed separately for spirals and early-type galaxies, the corresponding distributions being shown in left hand frames). For each galaxy its angular size was calculated, and the

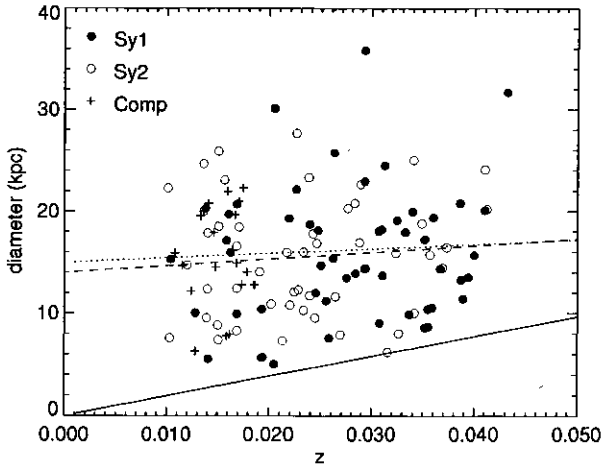

Fig. 11. Linear measured diameter (without Holmberg's correction) vs. redshift for Seyferts, and for nearby comparison galaxies with known z. The dotted and dashed lines show the least-square lines for Seyfert 1 and 2 galaxies, respectively, while the full line indicates the diameter corresponding to 0.2 mm in POSS plate

linear diameters are shown in the right hand side frames as a function of angular size, together with a curve displaying the running mean. According to Holmberg's measurements $\langle D\rangle_0 \approx 12$ kpc for spirals (volume limited sample; we have corrected his measurements from $H_0 =$ 80 km s^{-1} Mpc^{-1} to $H_0 = 100$ km s^{-1} Mpc^{-1}; Holmberg corrected diameters). However, due to the Malmquist effect the mean for galaxies with a fixed angular size rises to $\langle D\rangle_{\rm gal} \approx 20$ kpc. The short rising part of the curve follows from the limited coverage of the z-space: if this is expanded the same constant value is obtained for smaller and smaller angular sizes. Also shown is the analytical estimate (dashed line), based on $\sigma_{\log D} = 0.44$ for Holmberg spiral distribution, being in close agreement with the simulated value. For early-type galaxies ($\sigma_{\log D} = 0.57$), the simulations yield very similar $\langle D\rangle_{\rm gal}$, in spite of the large difference in the used $\langle D\rangle_0$ (≈ 7.5 kpc). Notice also that due to the strongly non-gaussian distribution function the analytical correction for ellipticals underestimates the true correction.

It is encouraging that the above estimate, $\langle D\rangle_{\rm gal} \approx$ 20 kpc is consistent with the mean Holmberg diameter of our control galaxies with known redshift, being 21.1 kpc for spirals and 19.5 kpc for early-type galaxies. As the Malmquist effect is independent of the angular size, and as the comparison galaxies with known z represent an angular size limited sample fairly well, we can assume that the mean linear diameter of the whole comparison sample is also close to this value. Incidentally, the mean Holmberg diameter for our Seyferts is very close to this value, namely 21.5 kpc. This indicates, first of all that Seyfert's are on the average larger than for example typical spiral galaxies (by a factor of about 1.8 when compared with Holmberg's

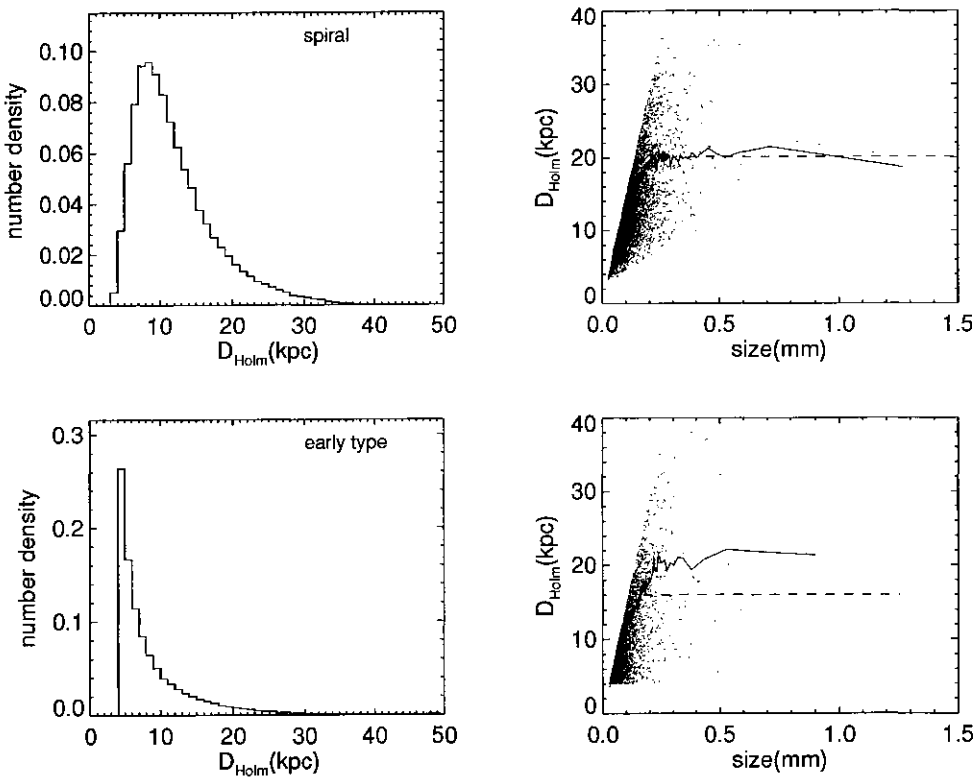

Fig. 12. Monte-Carlo simulation of Malmquist effect. In the left the Holmberg distribution function is shown separately for spirals and for early-type galaxies. In the right 100 000 galaxies with sizes drawn from these distributions have been placed randomly within the volume $z < 0.15$, and the resulting dependence between apparent size and true diameter is shown (for clarity, only 10 000 galaxies are displayed). Solid curve indicates the running mean of true diameter as a function of apparent diameter in simulations. Horizontal portion of the solid curve corresponds to the resulting mean linear size of a sample chosen according to apparent diameter criterion, rising portion is due to limited z-coverage. The dashed line indicates the analytical approximation, Eq. (7), calculated from the mean and standard deviation of the underlaying size distribution

mean diameter for spirals), and also that our selection, based on similar angular diameters, has picked up galaxies from the same part of the distribution function.

We can apply the above mean linear size estimate for our comparison galaxies to obtain a second estimate for the unknown redshifts, by assuming that all of them have linear Holmberg diameter of $D_{\rm gal} = 20$ kpc. Comparison between the estimates is shown in Fig. 13, plotting the new redshift based on a fixed linear size vs. the old one, based on the redshift of the corresponding Seyfert. Also shown are the galaxies with measured z (note that the dispersion for the galaxies with known z is only about 1/3 of that for the galaxies with unknown redshift). The mean assigned redshifts of the comparison sample (those without true redshift measurements) are 0.028 and 0.029 with the old and new method, respectively. In Paper II, both redshift estimates will be used.

5.3. *Absolute magnitudes*

The distance dependent Malmquist effect for Seyfert galaxies appears in the magnitude-redshift diagram, being similar for both Seyfert types (Fig. 14). The upper envelope in the figure is well understood by a limiting magnitude around 15.5 − 16.0 mag. However, the correlation between magnitudes and redshifts may not be the distance dependent Malmquist effect in the sense described in Sect. 5.2, being rather related to differences in Seyfert galaxy surface or nuclear brightnesses at different z. In fact, we don't see the same tendency for Seyfert galaxy diameters (see Fig. 11).

The parent galaxy brightnesses of Seyfert 1 galaxies by Granato et al. (1993), common with our sample Seyferts, are overestimated by 1.5 mag in comparison with the Holmberg's relationship between diameters and absolute magnitudes, yielding luminosities higher by a factor of 3–4. For comparison, the control galaxy luminosities at $z < 0.02$ are overestimated only by a factor of 1.6. This implies that our Seyfert galaxies should be much brighter than the comparison galaxies for a similar diameter range. However, closer inspection of our Seyfert sample reveals that the deviation from the Holmberg's relation $M_V - M_V(D_{\rm Holm})$ is strongly redshift dependent (Fig. 15) and that on the average the galaxies by Granato et al. have larger redshifts than our Seyferts. Seyferts at low red-

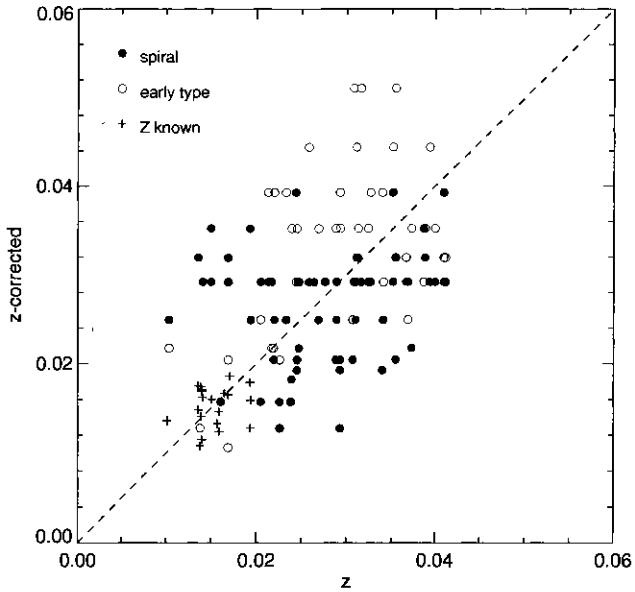

Fig. 13. Comparison between the two methods for estimating the unknown comparison galaxy redshifts: the abscissae indicate redshifts set indentical to the related Seyfert galaxies, while the ordinates are based on assuming that each galaxy has the Holmberg diameter of 20 kpc. Also shown (crosses) are comparison galaxies with known z: for these the ordinate corresponds to the measured redshift

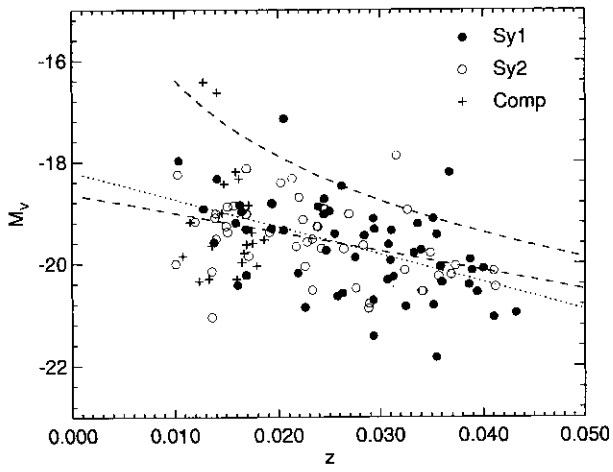

Fig. 14. Absolute visual magnitude vs. redshift for Seyferts, and for nearby comparison galaxies with known z. The dotted and dashed lines show the least-square lines for Seyfert 1 and 2 galaxies, respectively, while the curved dashed line corresponds to 16 mag apparent brightness

shifts roughly follow the Holmberg's relation, whereas at large distances galaxies with higher surface brightnesses, or with brighter nucleus, are selected (it is possible that the parent galaxy brightness is not well separated from the nuclear brightness for example due to scattering from dust in the parent galaxy disk). As there is no reason to assume that our comparison sample (chosen according to apparent diameter, not magnitude) would show similar M_V vs. z dependence, it most probably matches better with the low z Seyferts than with the high z Seyferts.

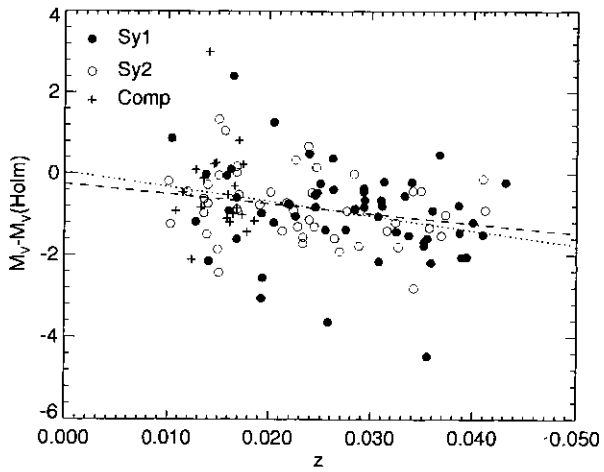

Fig. 15. Difference between galaxy absolute magnitude M_V and that derived from galaxy diameter via Holmberg relation $M_V\,(D_{\rm Holm})$, shown as a function of redshift. The dotted and dashed lines show the least-square lines for Seyfert 1 and 2 galaxies, respectively. For Seyferts, the deviation from the Holmberg relation increases with redshift, and reaches even 1.5 mags for large z. Also shown are comparison galaxies with known redshifts, following closely the empirical relation

The lack of the nuclear luminosities for our Seyfert galaxies complicates the comparison of Seyfert and control galaxy luminosities. Namely, as noticed in Sect. 2.2, a large fraction of the Seyfert galaxy luminosity may be nuclear nonthermal emission in origin, affecting significantly the total absolute magnitudes. According to Granato et al. the nuclear brightness exceeds 20% of the total galaxy brightness for the majority of Seyfert 1 galaxies, and is more than 50% for many Seyferts (the mean difference in M_V between the total and the parent galaxy brightnesses for the galaxies by Granato et al., common with in Fig. 15, is about 0.36). For comparison, the nuclear emission of normal galaxies is typically less than 1% of the total galaxy light (Minkovski 1968).

As we are interested in the host galaxy brightnesses the above arguments imply that the total absolute magnitudes of Seyferts and control galaxies cannot be used as a criterion for sample selection.

5.4. *Morphological types*

5.4.1. Principal samples

Galaxies of the principal Seyfert sample are divided into seven morphological classes (see Table 3; also comparison galaxies with known morphological type are shown) of which the first five follow the well known classification by de Vaucouleurs et al. (1976), while the class Irr-pec-S includes irregular galaxies, galaxies classified as spirals

without more detailed morphological characterization and peculiar galaxies. Those classified as "others" are largely compact (73% of Sy1 and 64% of Sy2), including also some pairs, groups and one merger. A galaxy with a well defined Hubble-type is kept in its original class even if it has an indication of some peculiarity. While excluding peculiar galaxies (Irr-pec-S and "others") the morphological distribution of our Seyferts follows the trend first emphasized by de Vaucouleurs (1974) who noticed that Seyferts are preferentially rather amorphous SO galaxies or early-type spirals. Later Whittle (1992) has pointed out that up to 30% of Seyferts may be late-type spirals.

The large fraction of distorted galaxies among Seyferts was first pointed out by Vorontsov-Velyaminov (1977) and Adams (1977) and was later confirmed by Wehinger & Wyckoff (1977) and Simkin et al. (1980). The connection between distorted morphology and tidal interaction for Seyferts has been later discussed by Mirabel & Wilson (1984) and MacKenty (1990). In our Seyfert sample 40% of the galaxies are somehow peculiar (Irr-pec-S and "others") in comparison with 23% among the control galaxies. These numbers are comparable with those found by Wehinger & Wyckoff and Mirabel & Wilson. It is possible that inspection of faint structures of these galaxies might show up spiral arms leading to the corresponding change in the classification.

Type 2 Seyferts are more often distorted than type 1 Seyferts (23% vs. 13%), while Seyfert 1 galaxies are more often Sb-ScI spirals (22% vs. 11%). The number of compact galaxies ("others") is almost equal among both Seyfert types. We do not confirm the trend found by Kachikian & Weedman (1971) who argued that Seyfert 1 galaxies are more often amorphous SO galaxies than type 2 Seyferts.

If we exclude peculiar objects (Irr-pec-S and "others") from the principal Seyfert sample, the control sample is somewhat biased towards early-type galaxies (E+SO). Additionally, early-type galaxies in the control sample are more often ellipticals than in the Seyfert sample. However, these comparisons are only tentative.

5.4.2. Other samples

The low redshift Seyfert sample is biased towards early-type galaxies (Table 2). This bias makes one to underestimate the number of companions at large distances, as earlier Hubble types live preferentially in regions of higher galaxy densities than galaxies of later types. In order to estimate the importance of this selection effect the mean number of physical neighbouring galaxies $N_{\rm comp}$ within a circle of 200 kpc in diameter was calculated for early- and late-type Seyferts in the redshift range $z = 0.01 - 0.02$. The value of $N_{\rm comp}$ was found to be approximately same (6.2 to 6.5) for both classes of morphological types. This difference is much less than the difference in $N_{\rm comp}$ between the low- and high redshift Seyferts, being 5.1 and 7.6, respectively.

Galaxies projected on Zwicky's clusters are more biased towards late-type galaxies than their non-projected counterparts, whereas type 1 and type 2 Seyferts have similar Hubble types.

5.5. *Distributions of Sy1 and Sy2 galaxies*

5.5.1. Principal sample

Figure 16 shows the cumulative number of type 1 and type 2 Seyferts as a function of redshift for our Seyfert sample. To the Class 1 we include also the intermediate type 1.5 galaxies and to the Class 2 types 1.8 and 1.9. This is reasonable, as Seyferts of type 1.5 still have strong broad components of their permitted emission lines, characteristic to type 1 objects. On the other hand, types 1.8 and 1.9 have strong, narrow, but very weak broad components of the H_α and H_β lines, being therefore more like Seyfert 2 galaxies. Both Seyfert samples are incomplete in spatial coverage, being however rather similar below the redshift 0.03. Beyond this distance, type 2 galaxies are underrepresented in comparison with type 1 objects. Kachikian & Weedman (1971) and (Yee 1983) pointed out that Seyfert 1 galaxies have higher nuclear-to-galaxy flux ratios when compared with Seyfert 2 galaxies. This explains why we have more Seyfert 1 galaxies at large distances.

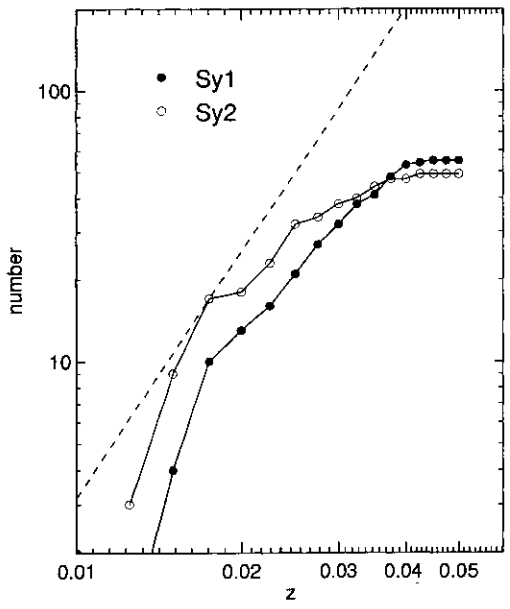

Fig. 16. Cumulative number of Sy1 and Sy2 galaxies in our sample as a function of redshift. The plot indicates that for $z < 0.03$ the relative fraction of the two activity classes is fairly constant, while for $z > 0.03$, Sy2 galaxies are strongly underrepresented. Dashed line indicates the relation with logarithmic slope -3, which would indicate complete spatial coverage

5.5.2. Other samples

The low redshift Seyfert sample has a small bias towards type 2 Seyferts (Table 2). If type 2 Seyferts have more companions than type 1 galaxies this implies that the number of neighbouring galaxies may be slightly overestimated for the low-redshift Seyferts. The Seyferts projected on Zwicky's clusters have the same fraction of Sy1/Sy2 as the non-projected Seyferts.

6. Cluster membership

Galaxy memberships in Zwicky's clusters (Zwicky 1961) and in Hickson's compact groups of galaxies (Hickson 1993) are shown in Table 4 for the Seyferts and for the low-redshift comparison galaxies ($z < 0.02$). By compact clusters Zwicky means galaxy associations where ten or more galaxies form a group, whereas Hickson's groups contain four or more galaxies. Additionally in Hickson's groups the faintest group member must not differ more than three magnitudes from the brightest member. Galaxy projections on nearby Zwicky's clusters at $v < 15\ 000$ km s^{-1} are marked in Col. 2. Zwicky's fields were not available for 25 Seyferts (13 Sy2 and 12 Sy1) and for 6 comparison galaxies, which reduced the numbers of Seyferts and the low-redshift comparison galaxies to 79 and 13, respectively. Cluster membership was confirmed using the redshift catalogue of the Center for Astrophysics Redshift Survey (Huchra et al. 1983). If redshifts were available for less than two galaxies in a cluster the cluster membership was considered uncertain. Distances from the cluster borders were calculated in two ways. First they were normalized to Zwicky's effective radius which gives the mean cluster size when circular shape is assumed (same as in Nesci 1986). As the shapes of the clusters are very irregular this normalizing method excludes many borderline galaxies falling outside Zwicky's effective radii. Secondly the distances were normalized to $r_1 + r_2$, where r_1 is the smallest distance from the cluster border and r_2 the distance from the cluster center.

In Table 5 the number distribution of Seyferts in different fields are shown and compared with the results by Nesci (1986) and Gisler (1978). We consider first projections on clusters. In our sample 64% of the Seyferts are field galaxies, whereas Nesci & Gisler found 55% and 50%, respectively. While considering non-projected Seyferts and those that are unphysical members of Zwicky's clusters (real memberships), as field galaxies, (excluding uncertain memberships) field Seyferts form the large majority, 80% of all Seyferts. If we include only Seyferts at $z < 0.03$ the corresponding value is 83% while excluding uncertain memberships, and 73% if they are taken into account.

The locations of the Seyferts in Zwicky's clusters are shown by Fig. 17 where they are compared with those obtained by Nesci, with the distributions of galaxies in spiral-rich clusters by Oemler, and with a uniform space distribution of galaxies. While using Nesci's normalizing method, results identical to this were obtained (filled circles in Fig. 17) showing that Seyferts have the same probability to be anywhere in the cluster. This contradicts Petrosian's (1982) result showing that Seyferts have the same space distribution as normal galaxies in clusters, coinciding twice more often with the central regions than with the cluster borders. However, while normalizing the distances to r_1+r_2 (diamonds in Fig. 17) Seyferts seem to be largely located at the cluster borders, as now also the borderline galaxies are included.

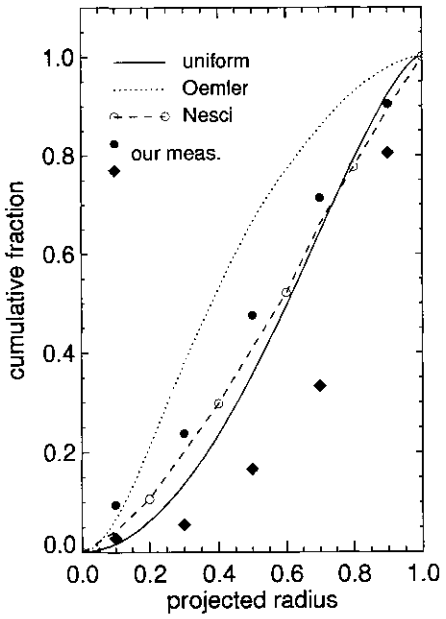

Fig. 17. Distribution of the projected Seyfert locations in the Zwicky's clusters for those Seyferts that were found to be physical cluster members. The symbols denote the two methods (explained in the text) for the calculations of projected radius in terms of the group radius. Filled dots are distances normalized to Zwicky's effective radii and filled diamonds those normalized to $r_1 + r_2$. For comparison the curves for uniform space distribution, Oemler-distribution and that found by Nesci (1986) are shown

We confirm the following results by Nesci:
1) Seyferts avoid compact clusters. However, contrary to Nesci Seyfert 1 and 2 galaxies have similar cluster environments.
2) Seyferts are distributed in clusters like Sc and later type galaxies rather than like SO-Sab objects (Nesci: Sb or later), when compared to Gisler's sample of 2004 galaxies from the Uppsala General Catalogue of Galaxies.

The Seyferts generally avoid Hickson's groups. However, three of them are members of the groups (Mrk176= H56B, NGC 7214=H91A, NGC 7319=H92C) implying that Seyfert activity can be triggered also in rather small groups of large galaxies, where the tidal effects are strong.

7. Summary

Samples of 104 Seyferts and 138 comparison galaxies (principal samples) were selected in the redshift range $z = 0.01 - 0.043$. The Seyferts are from the list of Dahari & de Robertis (1988) and the comparison sample was assembled from POSS plates using an apparent dimension criterion. Companions were counted within the circles of 1.5 Mpc in diameter to the photographic apparent magnitude limit of 19.1 $m_{\rm pg}$ (complete to about 18.9 $m_{\rm pg}$). Large measuring circles enable accurate elimination of background galaxies essential in the tests applied. The total number of counted galaxies is 23 284, being about 15 times more than in any of the previous works.

We discuss the possible selection effects involved. For example, the number of background galaxies is strongly redshift dependent, whereas the fraction of physical companions is rather uniform throughout the z-interval covered by the samples. This stresses the importance of good elimination of background galaxies. Due to the Malmquist effect and the distance-dependent Malmquist bias it is not selfevident that the Seyfert and the comparison samples should match both in diameter and magnitude: the Seyfert sample is a magnitude limited sample, whereas the comparison sample is diameter limited. In our Seyfert sample the distance dependent Malmquist effect is insignificant in diameter but important in absolute magnitude, implying that at large redshifts Seyferts deviate more from the Holmberg relation.

For the comparison sample the most important problem is that the redshifts are largely unknown. To estimate the redshift errors Monte-Carlo simulations were performed using Holmberg's diameter function and taking into account the Malmquist effect to obtain an independent estimate for true galaxy sizes in angular size limited sample. In this manner, mean Holmberg diameters were found to be 20 kpc both for spiral and early-type comparison samples. For spirals this estimate agrees with the analytical estimate based on Lynden-Bell formula, due to their centrally peaked size distribution. However, for early-type galaxies with strongly non-gaussian distribution the analytical formula underestimate the mean size in comparison to simulated value. The mean redshift obtained by assuming 20 kpc size for each galaxy was found to be equal to that estimated from the redshifts of the Seyfert galaxies, implying that our redshift estimates for the comparison galaxies are reasonable. Redshifts derived with both methods are used in the analysis of Paper II.

In the principal Seyfert sample type 1 and type 2 Seyferts are rather homogeneously distributed at $z < 0.03$, beyond which Seyfert 1 galaxies dominate. Morphological selection is more difficult to take into account, because 40% of the Seyferts in our sample are somehow peculiar. This renders accurate matching of morphological types meaningless unless similar morphological types are compared. In addition to the principal samples suitable subsamples were selected in order to test the methods by Dahari (1984) and FWS, as well as to check how much cluster properties affect the results concerning near neighbourhoods of galaxies.

We found that about 73– 83% of the Seyferts are field galaxies, which is significantly more than 55% suggested by Nesci. Seyferts were found to live preferentially at the cluster borders. We also confirm the earlier results showing that Seyferts avoid compact clusters and that they are distributed to clusters like late-type spirals (Sc or later). Three of the Seyferts are members of Hickson's groups.

Acknowledgements. Anticipating the results by Petrosian (1982) and MacKenty (1989), that Seyfert 2 galaxies have more companions than type 1 Seyferts, a small-scale study of Seyfert environments was performed by Mr. Matti Ojanen under the quidance of P. Teerikorpi around 1979 when the latter was working in the Observatory of Helsinki University. Matti Ojanen was actually a professional air captain serving the Finnish civil aviation, wishing to enlarge his view of the world by studies in astronomy. Several years after the quite untimely death of Matti Ojanen, the present, more extensive study was started, now in Tuorla Observatory. In the study of 1979, counts of galaxies were made in small circles ($r < 100$ kpc) around 46 Seyferts, in order to detect a possible concentration of true companions. In the short report (unpublished) one can read that "one gets the impression that Sy2 objects may be associated with small groups of galaxies more often than those of Class 1".

This research has made use of the NASA/IPAC Extragalactic Database (NED), which is operated by the Jet Propulsion Laboratory, California Institute of Technology, under contract with the National Aeronautics and Space Administration. We thank the referee, Dr. L. Danese for his valuable comments.

References

Adams T.F. 1977, ApJS 33, 19
Bushouse H.A. 1986, AJ 91, 255
Dahari O. 1984, AJ 89, 966
Dahari O. 1985, ApJS 57, 643
Dahari O., de Robertis M.M. 1988, ApJ 331, 727
de Vaucouleurs G. 1974, IAU Symposium 58, Formation and Dynamics of Galaxies, ed. J.R. Shakeshaft (Dordrecht: Reidel) 335
de Vaucouleurs G., de Vaucouleurs A. and Corwin H.G. 1976, Second Reference Catalogue of Bright Galaxies (Austin: University of Texas) (RCGB II)
Fuentes-Williams T., Stocke J.T. 1988, AJ 96, 1235
Gisler G.R. 1978, MNRAS 183, 633

Granato G.L., Zitelli V., Bonoli L., Danese L., Bonoli C., Delpino F. 1993, ApJS 89, 35
Heckman T. 1978, PASP 90, 241
Hickson P. 1993, Ap Letters 29, Vol. 1-3
Holmberg E. 1975, Galaxies and the Universe, in Stars and Stellar Systems, Vol. IX, Galaxies and the Universe, eds. A. Sandage, M. Sandage and J. Kristian, p. 123
Huchra J., Davis M., Latham D., Tonry J. 1983, ApJS 52, 89
Kachikian E., Ye Weedman D.W. 1971, Afz 7, 389
Karachentsev J.D., Karachentseva V.E., Shapovalova A.J., Jaakkola T. 1972, SvA 15, 728
Keel W.C., Kennicutt R.C., Hummel E., van der Hulst J.A. 1985, AJ 90, 708
Kotilainen J., Ward M.J., Williger G.M. 1993, MNRAS 263, 655
Lake G., Tremainel S. 1980, ApJ 238, L13
Laurikainen E., Salo H., Aparicio A. 1993, ApJ 410, 574
Laurikainen E., Salo H. 1994, A&A, in press (Paper II)
Lynden-Bell D., Faber S.M., Burstein D., Davies R.L., Dressler A., Terlevich R.J., Wegner G. 1988, ApJ 326, 19
MacKenty J.W. 1989, ApJ 343, 125
MacKenty J.W. 1990, ApJS 72, 231
Mazzarella J.M., Balzano V.A. 1986, ApJS 62, 751
Minkovski R. 1968, AJ 73, 842
Mirabel I.F., Wilson A.S. 1984, ApJ 277, 92
Nesci R. 1986, A&A 160, 259
Nilson P. 1973, Uppsala General Catalogue of Galaxies (Uppsala Offset Center, Uppsala)
Osterbrock D.E. 1984, QJRAS 25, 1
Osterbrock D.E. 1993, ApJ 404, 551
Paturel G., Fougue P., Bottinelli L., Gougenheim L. 1989, Catalogue of Principal Galaxies (Lyon, France)
Petrosian A.R. 1982, Afz 18, 548
Schombert J.M., Wallin J.F., Struck-Marcell C. 1990, AJ 99, 497
Shane C.D. 1975, Galaxies and the Universe, in Stars and Stellar Systems, Vol. IX, eds. A. Sandage, M. Sandage and J. Kristian, 647
Shuder J.M., Osterbrock D.E. 1981, ApJ 250, 55
Simkin S.M., Su H.J., Schwarz M.P. 1980, ApJ 237, 404
Terlevich R., Melnick J. 1985, MNRAS 213, 841
Vorontsov-Velyaminov B.A. 1977, A&AS 28, 1
Weedman D.W. 1977, ARA&A 15, 69
Weedman D.W. 1978, MNRAS 184, 11p
Wehinger P.A., Wyckoff S. 1977, MNRAS 181, 211
Whittle M. 1992, ApJS 79, 49
Yee M.K.C. 1983, ApJ 272, 473
Zwicky F., Herzog E., Wild P. 1961, Catalogue of Galaxies and Clusters of Galaxies (California Institute of Technology)

1994A&AS..108..491L

Table 1. The samples

Galaxy name (1)	z (2)[3,4,5]	T_m (3)[1,2,3,4,5]	T_{Sy} (4)[6]	m_v (5)[3]	D_{meas} (mm) (6)	$D_{major} \times D_{minor}$ (arcmin) (7)[3,7]	b/a (8)
Seyferts ($z < 0.043$)							
Mrk3	0.0139	S	2.0	14.0	0.70	1.8x1.6	0.89
Mrk9	0.0400	SO/pec	1.0	15.3	0.40	0.5x0.4	0.80
Mrk10	0.0293	SBbc	1.0	13.3	1.25	1.9x0.7	0.37
Mrk40	0.0205	SO/pec	1.0	16.8	0.25	1.3x0.2	0.15
Mrk42	0.0245	SBb	1.0	15.3	0.50	0.5x0.4	0.80
Mrk79	0.0219	SBc	1.5	13.9	0.90	1.2x1.2	1.00
Mrk110	0.0352	pair	1.0	16.0	0.25	0.5x0.2	0.30
Mrk141	0.0387	E	1.5	15.4	0.35	0.3x0.3	0.83
Mrk176	0.0269	group	2.0	15.5	0.30	1.1x0.6	0.55
Mrk198	0.0239	SO/pec	2.0	15.0	0.50	0.8x0.8	1.00
Mrk231	0.0410	Sc/pec	1.0	14.4	0.50	1.7x1.1	0.65
Mrk266	0.0276	compact	2.0	14.1	0.75	1.2x1.1	0.92
Mrk268	0.0410	pair	2.0	15.3	0.60	0.9	0.60
Mrk270	0.0103	SABO	2.0	14.2	0.75	1.1x1.0	0.91
Mrk273	0.0369	pec	2.0	15.0	0.40	1.2x0.3	0.21
Mrk279	0.0307	SO	1.5	14.5	0.60	0.9x0.5	0.56
Mrk290	0.0308	E	1.5	15.2	0.30	0.5	0.86
Mrk308	0.0233	IO	2.0	14.7	0.45	0.7	0.65
Mrk315	0.0394	E/pec	1.5	14.8	0.35	0.6	0.82
Mrk334	0.0217	pec	1.8	14.4	0.75	1.0x0.7	0.70
Mrk335	0.0258	SOa	1.0	13.8	0.30	0.3x0.3	1.00
Mrk348	0.0151	SO	2.0	13.9	0.50	1.6x1.5	0.94
Mrk352	0.0141	SO	1.0	14.8	0.40	0.8x0.4	0.50
Mrk358	0.0360	SBbc	1.0	14.8	0.55	0.7x0.7	1.00
Mrk359	0.0169	SBOa	1.5	14.2	0.60	0.7x0.5	0.71
Mrk372	0.0310	SOa	1.5	14.9	0.60	0.9	0.81
Mrk382	0.0340	SBc	1.0	15.3	0.60	0.8x0.7	0.88
Mrk403	0.0244	compact	2.0	15.4	0.40	0.5x0.4	0.90
Mrk417	0.0327	compact	2.0	16.0	0.25	0.5	0.87
Mrk423	0.0324	SOa	1.8	14.8	0.50	0.9x0.5	0.56
Mrk471	0.0341	SBa	1.8	14.5	0.75	0.9x0.5	0.56
Mrk474	0.0355	SBOa	1.0	15.7	0.30	1.3x0.6	0.46
Mrk477	0.0373	compact	2.0	15.2	0.45	0.7	0.73
Mrk486	0.0389	compact	1.0	15.2	0.30	0.5	0.60
Mrk493	0.0313	SBb	1.0	14.6	0.80	1.3x1.3	1.00
Mrk504	0.0367	SB	1.0	17.0	0.40	0.3x0.2	0.67
Mrk509	0.0355	compact	1.5	13.3	0.25	0.5	0.85
Mrk522	0.0316	compact	2.0	17.0	0.20	0.2x0.2	1.00
Mrk530	0.0293	Sb/pec	1.5	14.0	0.80	1.4x0.9	0.64
Mrk533	0.0289	SBbc/p	2.0	13.9	0.80	1.0x0.9	0.90
Mrk543	0.0255	compact	1.0	15.0	0.45	0.4x0.4	1.00
Mrk573	0.0171	SBO	2.0	13.7	1.10	1.7x1.6	0.94
Mrk590	0.0263	SO	1.5	13.9	1.00	1.3x1.3	1.00
Mrk595	0.0275	compact	1.0	14.7	0.50	0.8	0.63
Seyferts (continued)							
Mrk609	0.0342	Im/pec	1.8	14.5	0.30	0.4x0.3	0.75
Mrk612	0.0202	SBOa	2.0	15.5	0.55	0.8x0.5	0.63
Mrk622	0.0288	S	2.0	14.6	0.55	0.6x0.6	1.00
Mrk686	0.0140	SBb	2.1	13.6	1.30	1.6x1.1	0.69
Mrk699	0.0337	compact	1.0	15.8	0.30	0.2x0.2	1.00
Mrk704	0.0294	S	1.5	15.4	0.50	0.7x0.4	0.57
Mrk728	0.0357	compact	1.8	14.9	0.45	0.7	0.66
Mrk739	0.0284	S	1.0	15.2	0.50	0.5X0.5	1.00
Mrk766	0.0128	SBa	1.5	14.0	0.80	0.9x0.9	1.00
Mrk871	0.0333	SBO	1.5	15.2	0.55	0.6x0.3	0.50
Mrk885	0.0250	Sab	1.5	15.4	0.60	0.7x0.4	0.57
Mrk896	0.0262	pair	1.0	16.0	0.60	1.1x0.8	0.55
Mrk915	0.0239	S	1.5	15.4	0.80	1.0x0.3	0.30
Mrk917	0.0242	SBa	2.0	14.6	0.75	1.1x1.1	1.00
Mrk928	0.0224	Sab/pec	2.0	15.0	0.55	0.9	0.75
Mrk938	0.0191	pair	2.0	14.4	0.75	2.2x0.8	0.36
Mrk955	0.0349	SB	2.0	15.3	0.55	0.7x0.4	0.57
Mrk993	0.0151	Sa	2.0	14.4	1.75	2.6x0.8	0.31
Mrk1040	0.0165	Sbc	1.5	14.5	2.50	4.5x1.3	0.29
Mrk1044	0.0163	S	1.0	14.6	1.00	0.7x0.6	0.86
Mrk1048	0.0432	pair	1.5	14.6	0.75	1.1	0.77
Mrk1058	0.0169	SB	2.0	15.4	0.75	0.7x0.4	0.57
Mrk1066	0.0120	SBO	2.0	13.6	1.25	2.0x1.5	0.75
Mrk1073	0.0233	SBb	2.0	13.7	0.70	1.0x0.9	0.80
Mrk1095	0.0325	Sb/pec	1.0	14.1	0.60	1.4x1.0	0.71
Mrk1098	0.0359	compact	1.5	15.1	0.30	0.3x0.2	0.80
Mrk1126	0.0104	SBa	1.5	14.5	1.50	1.8x1.8	1.00
Mrk1146	0.0386	Sab	1.0	14.9	0.55	1.0x0.6	0.60
Mrk1157	0.0151	SBOa	2.0	13.9	1.25	1.4x1.1	0.79
Mrk1218	0.0283	S	1.8	15.0	0.75	0.8x0.4	0.50
Mrk1239	0.0194	compact	1.0	15.0	0.30	0.5	0.80
Mrk1243	0.0352	Sa	1.0	14.3	0.50	1.0x0.9	0.90
Mrk1310	0.0193	compact	1.0	14.5	0.30	0.5	0.62
Mrk1388	0.0213	compact	2.0	15.7	0.35	0.6	1.00
Mrk1400	0.0293	SO	1.0	15.6	0.50	0.8	0.42
Mrk1469	0.0311	SBb	1.5	15.5	0.45	0.8x0.3	0.38
NGC1144	0.0288	B/pec	2.0	13.8	0.60	1.4x1.2	0.86
NGC1241	0.0136	SBb/p	2.0	12.0	1.85	2.8x1.7	0.61
NGC1410	0.0246	E/pec	2.0	15.4	0.70	1.2x1.2	1.00
NGC4074	0.0220	SO/p	2.0	15.4	0.50	0.4x0.2	0.57
NGC4922	0.0238	IO/p	2.0	15.0	1.00	2.3x1.0	0.43
NGC5135	0.0136	SBab	2.0	12.9	1.50	2.6x1.8	0.69
NGC5548	0.0169	SOa	1.5	13.3	1.25	1.4x1.3	0.88
NGC5728	0.0101	Sa	2.0	12.4	2.25	3.1x1.8	0.58
NGC6423	0.0245		1.0	15.6	0.50	0.3x0.2	0.80
NGC7212	0.0264	merger	2.0		0.45	1.6x0.7	0.44
NGC7214	0.0226	SBbc/pec	1.0	13.3	1.00	2.2x1.4	0.64
NGC7319	0.0226	Sbc/p	2.0	14.1	1.25	1.6x1.2	0.75

1994A&AS..108..491L

Table 1. continued

Galaxy name	z	T_m	T_{Sy}	m_v	D_{meas}	$D_{major} \times D_{minor}$	b/a
Seyferts (continued)							
NGC7469	0.0161	SBa	1.5	13.0	1.25	1.6x1.1	0.69
Akn79	0.0140	S	2.0	14.1	0.90	0.8x0.2	0.24
Akn539	0.0169	E	2.0	15.4	0.50	0.3x0.3	1.00
Akn564	0.0247	SB	1.0	14.6	0.75	0.7x0.4	0.57
IC4329	0.0159	SO	1.0	14.2	1.10	0.6	0.16
MCG81111	0.0205	S	1.5	14.6	1.50	2.1	0.89
0438 – 084	0.0150	SBab	2.0	14.0	0.60	1.2x0.8	0.67
0450 – 032	0.0157	SBOa	2.0	14.5	1.50	1.3x0.9	0.67
1249 – 131	0.0138	SBOa	1.5	13.5	1.50	1.8x0.7	0.39
1319 – 164	0.0169		2.0	14.5	1.00	1.0x0.8	0.80
1423 – 116	0.0412		2.0	15.0	0.50	0.5x0.4	0.80
Comparison galaxies($z < 0.02$)							
late (Sa – S) :							
PGC17456	0.0141	Sc		16.5	1.50	1.7X0.3	0.17
PGC19776	0.0128	Sd		16.5	0.50	1.3X0.8	0.62
PGC21181	0.0179	Sa		13.6	0.80	1.0x0.8	0.80
PGC12259	0.0175	SBb/pec		14.0	1.30	1.5x1.1	0.73
PGC47255	0.0148	Scd/pec		14.8	1.00	1.7x0.4	0.24
PGC9314	0.0171	S		14.7	1.25	1.9x0.5	0.26
PGC9773	0.0169	Sb		13.9	0.90	1.7x1.1	0.65
PGC49580	0.0146	Sbc		14.2	1.25	1.7x0.3	0.17
early (E – S0a) :							
NGC4933B	0.0108	SOa/pec		12.7	1.50	1.8x0.8	0.44
PGC19328	0.0174	SO		14.2	0.75	1.2x0.9	0.75
PGC3564	0.0162	E		15.1	0.50	0.5x0.5	1.00
PGC27791	0.0159			15.2	0.50	0.4x0.4	1.00
PGC52916	0.0136	SO/pec		13.4	1.50	1.3x1.0	0.77
PGC47582	0.0124	E		12.5	1.00	1.9x1.8	0.95
PGC16508	0.0133	SO		12.7	1.50	1.5x1.1	0.73
PGC5299	0.0160	SO		13.1	1.40	2.4x2.1	0.88
PGC10810	0.0165	E		13.5	1.00	1.7x1.4	0.82
PGC8013	0.0167	SO		13.7	1.20	1.6x1.2	0.75
PGC51598	0.0115	E		13.5	1.30	1.6x1.1	0.69
PGC7090	0.0186	E		14.2	0.70	1.1x1.1	1.00

[1] Mazzarella and Balzano 1986
[2] de Vaucouleurs et al. 1976
[3] NASA/IPAC Extragalactic Data Base
[4] de Vaucouleurs et al. 1991
[5] Paturel et al. 1989
[6] Dahari and de Robertis 1988
[7] Nilson 1973

Table 2. The samples selected

Sample	N_{tot}	mean z	z – range	mean M_V	N_{Sy1}	N_{Sy2}	N_{early}	N_{late}	N_{pec}
Sy	104	0.0255	0.0101 – 0.0432	−19.6	55	49	29	29	43
Sy1	55	0.0275	0.0104 – 0.0432	−19.7			17	16	21
Sy2	49	0.0233	0.0101 – 0.0412	−19.5			12	13	22
$Sy_{high\ z}$	58	0.0307	0.0233 – 0.0400	−19.8	36	22	13	16	28
$Sy_{low\ z}$	60	0.0193	0.0101 – 0.0269	−19.3	26	34	20	16	22
Sy_{proj}	29	0.0260	0.0120 – 0.0410	−19.4	15	14	6	10	12
$Sy_{non-proj}$	50	0.0265	0.0103 – 0.0410	−19.6	28	22	17	11	22

Table 3. Morphological types of Seyferts

Type	N_{Sy}	N_{Sy}(%)	N_{Sy1}	N_{Sy1}(%)	N_{Sy2}	N_{Sy2}(%)	N_{comp}	N_{comp}(%)
E – ESO	5	5.0	3	5.5	2	4.2	6	20.0
SO – SOa	26	25.7	15	27.8	11	23.4	7	23.0
Sa – Sab	13	12.9	6	11.1	7	14.9	2	6.7
Sb – Sbc	14	13.9	9	16.0	5	10.6	5	15.6
Sc – Scl	3	3.0	3	5.6	–		3	10.0
Irr – pec – S	18	17.8	7	13.0	11	23.4	6	20.0
Others	22	21.8	11	20.4	11	23.4	1	3.0
Total	101		54		47		30	

1994A&AS..108..491L

Table 4. Galaxy membership in Zwicky's clusters

Gal	proj	conf(N)	Zwicky cluster	r_1	r_2	Hickson group
Seyferts						
Mrk3	near	+(4)	MC501 : 0107.5 + 3212	0.52	0.93	
Mrk10	near	−(7)	MC286 : 0733.4 + 6102	0.71	0.70	
Mrk40	near	−(7)	MC268 : 1138.7 + 5650	1.00	1.00	
Mrk79	near	+(3)	MC235 : 0739.8 + 4949	0.13	0.19	
Mrk176	near	−(7)	MC268 : 1138.7 + 5650	0.92	0.99	56B
Mrk268	near	+(11)	MC161 : 1339.9 + 3030	0.31	0.42	
Mrk352	near	+(4)	MC501 : 0107.5 + 3212	0.91	0.87	
Mrk358	near	−(24)	MC502 : 0107.5 + 3212	1.30	0.94	
Mrk382	near	−(1)	O207 : 0745.5 + 4020	1.24	0.84	
Mrk417	near	+(1)	O125 : 1048.6 + 2358	0.53	0.77	
Mrk423	near	+(1)	O185 : 1123.9 + 3541	0.17	0.26	
Mrk493	near	(0)	MC195 : 1552.6 + 3435	1.14	0.85	
Mrk504	near	+(14)	O169 : 1701.4 + 2830	0.75	0.72	
Mrk533	near	−(19)	MC406 : 2320.0 + 0845	0.56	0.75	
Mrk595	near	+(4)	O414 : 0240.6 + 0740	0.42	0.59	
Mrk622	near	−(3)	O207 : 0801.3 + 3954	1.20	0.89	
Mrk699	near	+(25)	MC224 : 1625.5 + 4006	0.91	0.97	
Mrk704	near	+(5)	O91 : 0909.7 + 1814	0.77	0.87	
Mrk728	near	+(4)	MC66 : 1058.6 + 1049	1.10	0.93	
Mrk993	near	+(18)	MC502 : 0107.5 + 3212	1.28	0.92	
Mrk1040	near	+(14)	O504 : 0226.0 + 2600	1.10	0.90	
Mrk1066	near	+(5)	MC524 : 0303.0 + 4125	70	0.88	
Mrk1218	near	+(3)	O120 : 0837.0 + 2506	0.38	0.50	
Mrk1469	near	−(9)	MC269 : 1138.7 + 5650	2.40	1.00	
NGC4074	near	+(3)	O98 : 1202.0 + 2028	0.37	0.50	
NGC4922	near	+(45)	C160 : 1257.1 + 2806	0.58	0.76	
NGC6423	near	+(1)	MC321 : 1745.6 + 6703	1.65	0.97	
NGC7469	near	−(1)	O405 : 2259.6 + 0746	0.63	0.76	
Akn539	near	+(1)	MC254 : 1916.8 + 4855	1.80	1.00	
Comp. (S) $z < 0.02$:						
PGC9773	near	+(15)	MC539 : 0303.0 + 4125	1.18	0.91	
Comp. (early) $z < 0.02$:						
PGC5299	near	+(3)	MC521 : 0107.5 + 3212	1.50	0.98	
PGC10810	near	+(6)	MC524 : 0303.0 + 4125	0.78	0.93	
PGC8013	near	+(2)	MC504 : 0150.9 + 3050	1.30	0.97	

The following Seyferts are not projected to clusters: Mrk 6, Mrk 9, Mrk 42, Mrk 110, Mrk 141, Mrk 198, Mrk 231, Mrk 266, Mrk 270, Mrk 273, Mrk 279, Mrk 290, Mrk 308, Mrk 315, Mrk 334, Mrk 335, Mrk 348, Mrk 359, Mrk 372, Mrk 403, Mrk 471, Mrk 474, Mrk 477, Mrk 486, Mrk 522, Mrk 543, Mrk 573, Mrk 686, Mrk 739, Mrk 766, Mrk 871, Mrk 885, Mrk 917, Mrk 955, Mrk 1058, Mrk 1073, Mrk 1098, Mrk 1146, Mrk 1157, Mrk 1239, Mrk 1243, Mrk 1310, Mrk 1388, Mrk 1400, NGC 5548, NGC 7212, NGC 7319, Akn 79, Akn 564, MCG 81111.

The non-projected comparison galaxies are: PGC 17456(S), PGC 19776(S), PGC 21181(S), PGC 9314(S), PGC 19328(early), PGC 3564(early), PGC 27791(early), PGC 51598(early), PGC 7090(early).

Table 5. Number of Seyferts as a function of environment

Sample	Nesci projected N_{Sy1}	Nesci projected N_{Sy2}	Nesci projected N_{Sy1+2}	Gisler projected N_{Sy1+2}
Field	26 (52%)	16 (57%)	42 (55%)	14 (50%)
Open	11 (22%)	3 (11%)	14 (18%)	7 (25%)
Med.comp.	13 (26%)	9 (32%)	22 (28%)	7 (25%)
Comp.	0 (0%)	0 (0%)	0 (0%)	0 (0%)
Total	50 (100%)	28 (100%)	78 (100%)	28 (100%)

Sample	Our sample projected N_{Sy1}	Our sample projected N_{Sy2}	Our sample projected N_{Sy1+2}	Our sample real N_{Sy1}	Our sample real N_{Sy2}	Our sample real N_{Sy1+2}
Field	28 (67%)	22 (61%)	50 (64%)	34 (85%)	23 (70%)	57 (80%)
Open	6 (14%)	5 (14%)	11 (14%)	3 (8%)	2 (6%)	5 (7%)
Med.comp.	8 (19%)	8 (22%)	16 (20%)	3 (8%)	5 (15%)	8 (11%)
Comp.	0 (0%)	1 (3%)	1 (1%)	0 (0%)	1 (3%)	1 (1%)
Total	42 (100%)	36 (100%)	78 (100%)	40 (100%)	33 (100%)	71 (100%)